

# **Protein Amyloid Fibrils as Template for the Synthesis of Silica Nanofibers, and their use to prepare superhydrophobic, lotus-like surfaces**

## **Supporting Information**

Simonetta Rima and Marco Lattuada \*

Department of Chemistry, University of Fribourg, Chemin du Musée 9, CH-1700, Fribourg

\*Corresponding Author: Prof. Marco Lattuada ([marco.lattuada@unifr.ch](mailto:marco.lattuada@unifr.ch))

The following SI includes: a general characterization of protein amyloid fibrils (AFM image in Figure S1, zeta-potential measurements in Figure S2); one SEM image of the amyloid fibrils (1mg/mL) incubated for 12h with TMOS at pH 3.0 in Figure S3, several SEM images of silica fibers prepared via hydrolysis-condensation of TEOS in Stöber process for different conditions in Figure S4 and S5, an SEM comparison between Lotus leaf nanotubules and silica nanotubes in Figure S6, some SEM images of Lotus leaf, with and without wax nanotubules in Figure S7, SEM images of substrates with SCCs and BCCs in Figure S8, SEM images of early stages LbL deposition of silica fibrils on the surface of the BCCs in Figure 9, a schematic of the numerical approach used to compute the water contact angle on a flat surface, shown in Figure S10, and the contact angle measurement of a surface coated with non-hydrophobized silica nanotubes.

Figure S1

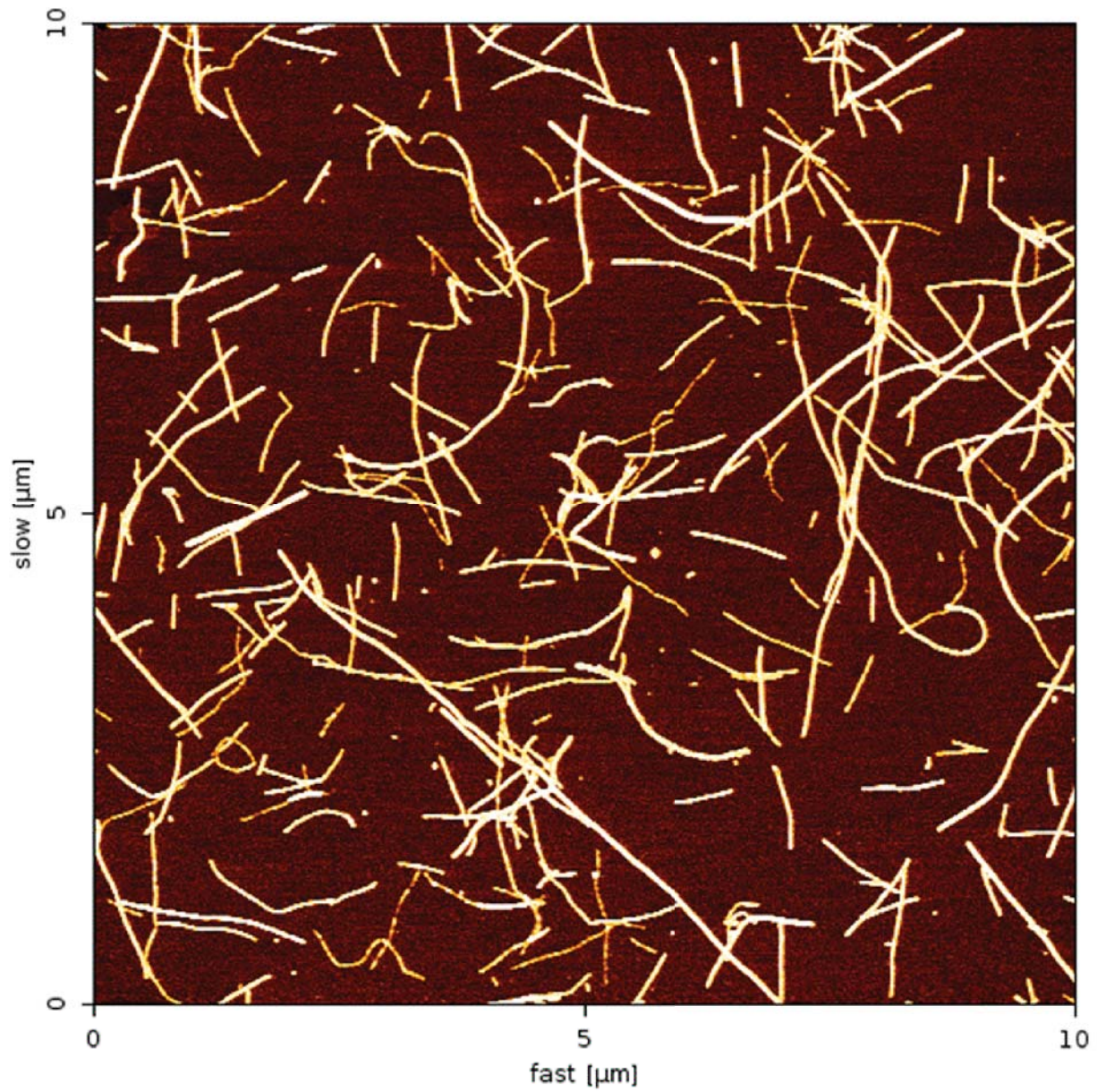


Figure S1. AFM picture of amyloid fibrils prepared from 10 mg/ml  $\beta$ -lactoglobulin incubated in 10 mM of HCl at 80°C. Scan size of the AFM pictures 10 $\mu$ m x 10 $\mu$ m.

Figure S2

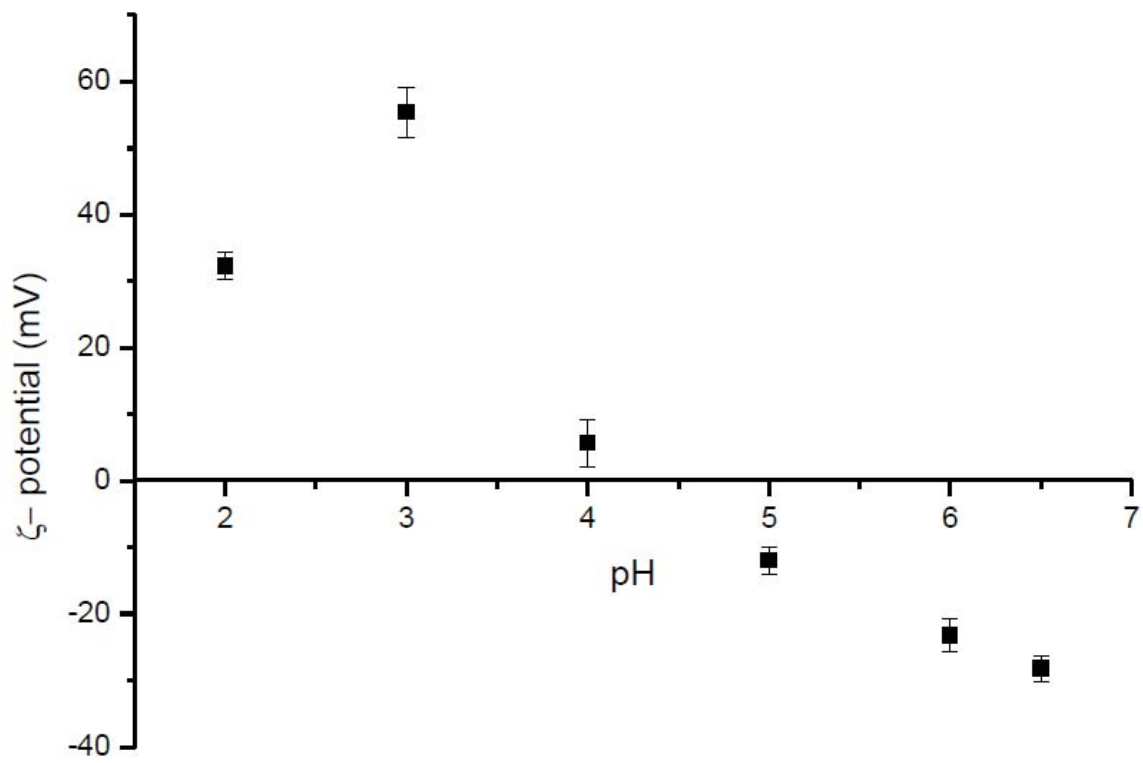


Figure S2.  $\zeta$ -potential of 10 mg/ml  $\beta$ -lactoglobulin fibrils incubated in 10 mM of HCl at 80°C in the pH range 2.0-6.5.

**Figure S3**

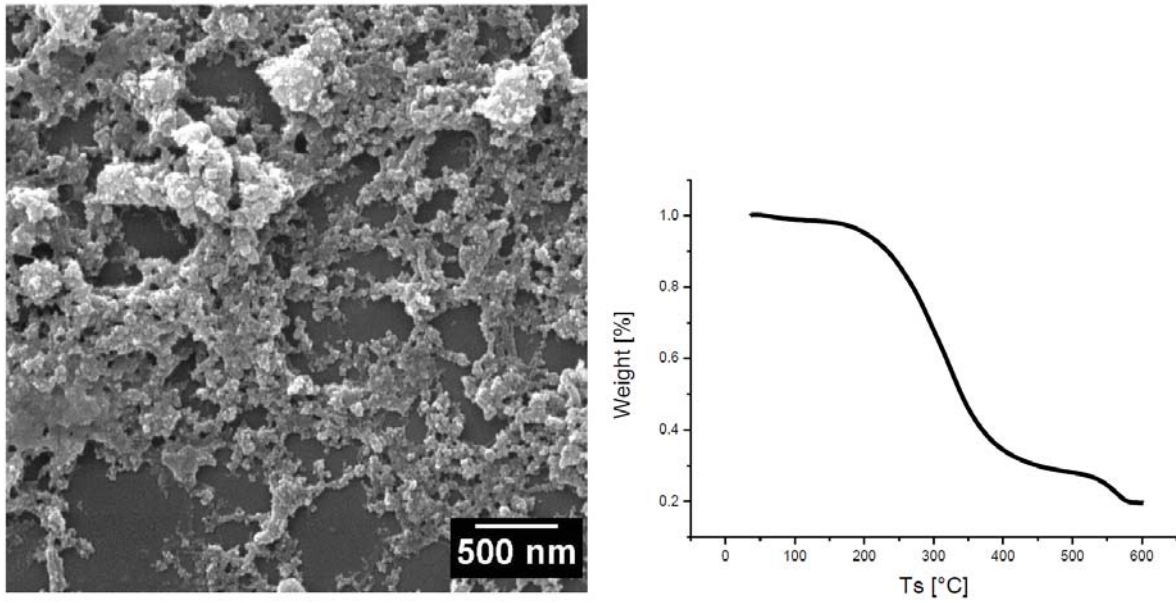


Figure S3. Left, SEM picture of amyloid fibrils (1mg/mL) incubated for 12h with TMOS at pH 3.0. Right, Thermogravimetric analysis of naked amyloid fibrils.

Figure S4

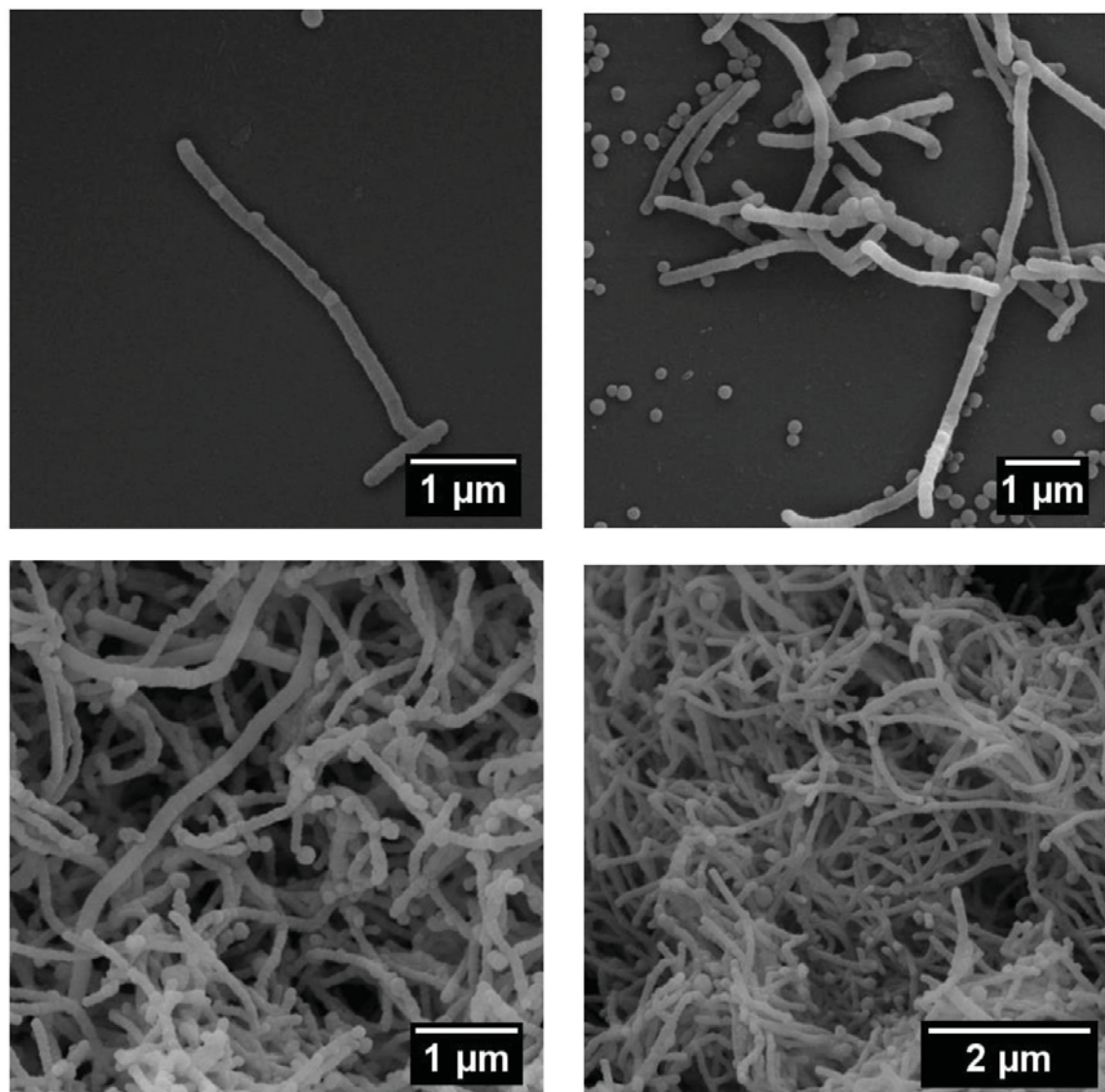


Figure S4. SEM images of silica nano-fibers obtained from the hydrolysis-condensation of TEOS, for one condition reported in Table 2 in the main paper. Sample: SF<sub>p</sub>-5 (semi-batch process, 1/1 TEOS/ammonia ratio, 500μL TEOS).

**Figure S5**

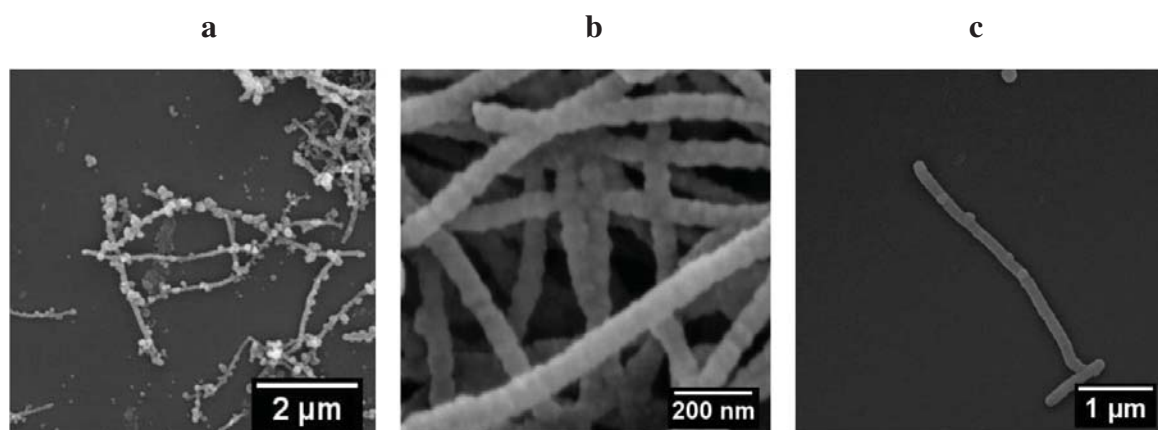
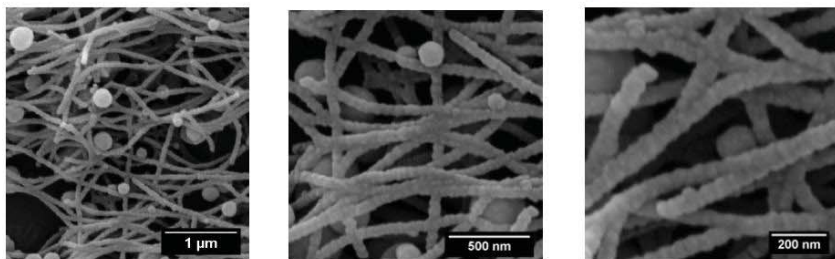


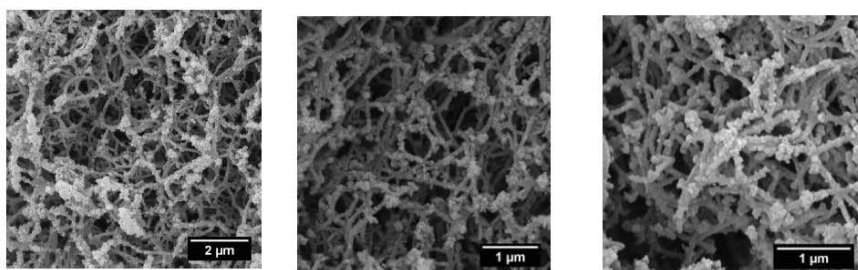
Figure S5. SEM images of silica nano-fibers for the samples reported in Table 2: (a) SF<sub>p</sub>-6 (100μL TEOS, 100μL ammonia, semi-batch process), (b) SF<sub>p</sub>-11 (500μL TEOS, 200μL ammonia, semi-batch process), (c) SF<sub>p</sub>-5 (500μL TEOS, 500μL ammonia, semi-batch process).

**Figure S6**

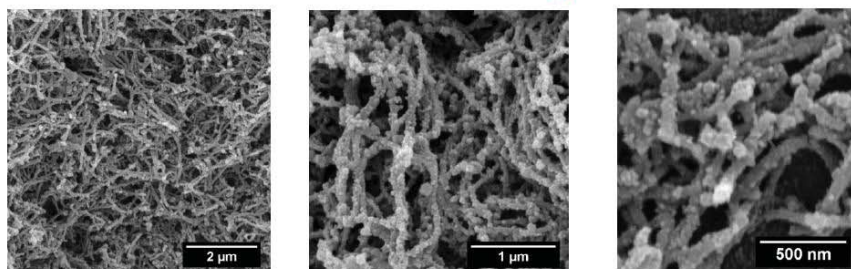
EtOH 9mL, Fibrils 1mL [10g/L], TEOS 500 $\mu$ L, **NH<sub>3</sub> 200 $\mu$ L**, SEMI-Batch process



EtOH 9mL Fibrils 1mL [10g/L] TEOS 500 $\mu$ L **NH<sub>3</sub> 100 $\mu$ L** SEMI-Batch process



EtOH 9mL Fibrils 1mL [10g/L] TEOS 500 $\mu$ L **NH<sub>3</sub> 50 $\mu$ L** SEMI-Batch process



EtOH 9mL Fibrils 1mL [10g/L] TEOS 100 $\mu$ L **NH<sub>3</sub> 100 $\mu$ L** SEMI-Batch process

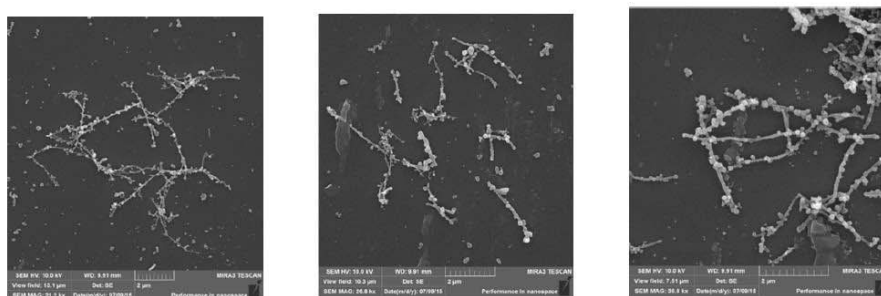


Figure S6. SEM images of silica nano-fibers obtained from the hydrolysis-condensation of TEOS carried out under different operating conditions.

**Figure S7**

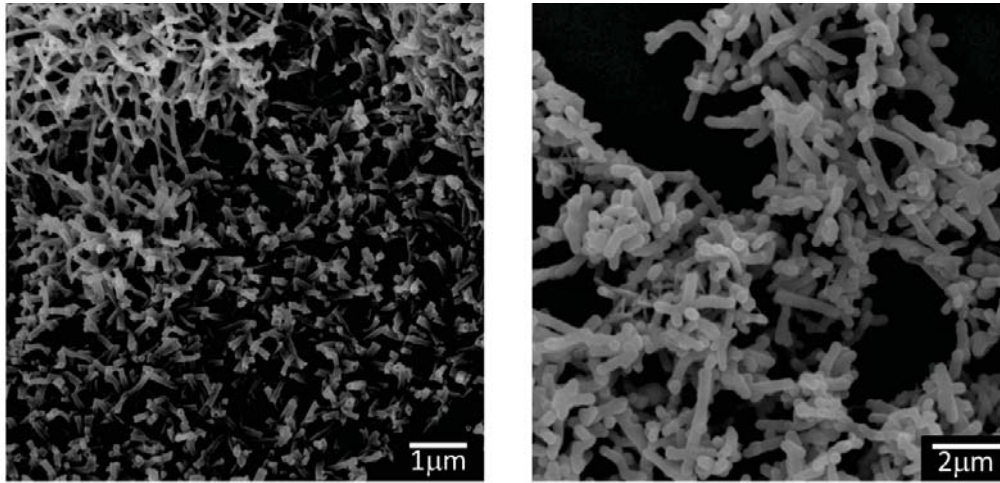


Figure S7. Left, SEM image of wax nanotubes on the surface of a lotus leaf. Right, SEM Image of the silica nanotubes, SF<sub>p</sub>-5, prepared in this work.



Figure S8

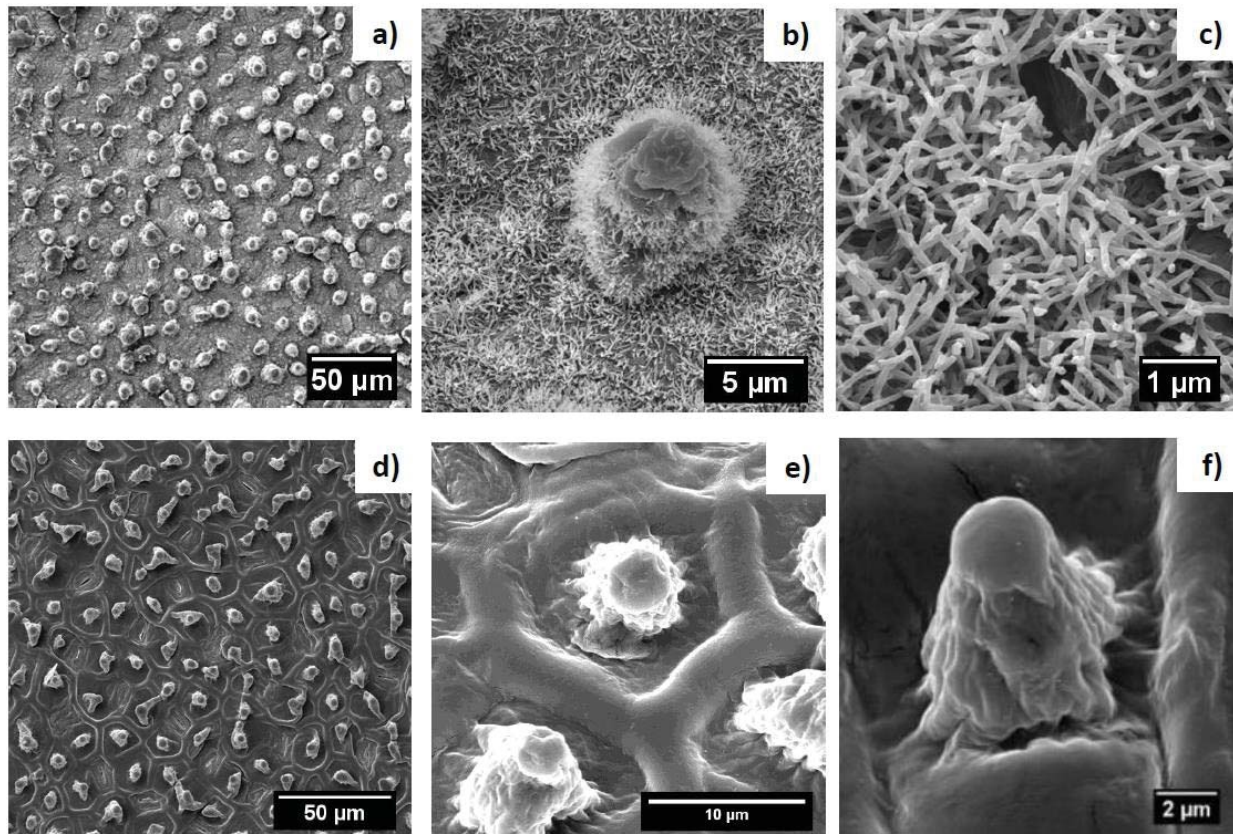


Figure S8. SEM images: (a, b, c) natural Lotus leaf, at three different magnifications (50μm, 5μm, 1μm); (d, e, f) natural Lotus leaf without the surface waxes, after being dipped in ethanol for 30 minutes to remove the wax crystals, at three different magnifications (50μm, 10μm, 2μm).

Figure S9

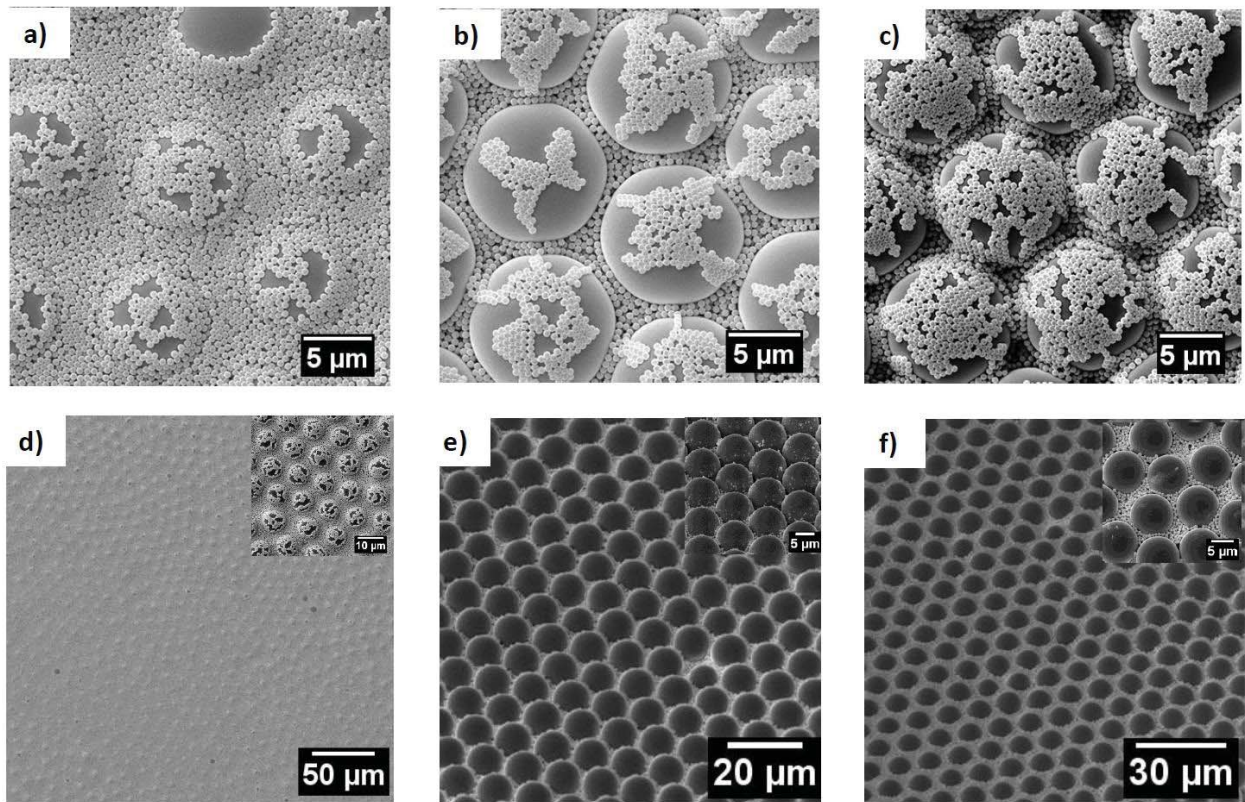


Figure S9. SEM images of BCCs structures. (a, b, c, d) BCCs surfaces of 10 μm and 500 nm PS particles for: (a and d)  $N_{S/L}$  equal to 1000; (b)  $N_{S/L}$  equal to 300; (c)  $N_{S/L}$  equal to 100. (e, f) BCCs structures of 10 μm and 750 nm magnetic particles. (e)  $N_{S/L}$  equal to 100 and (f)  $N_{S/L}$  equal to 500, at different magnifications.

**Figure S10**

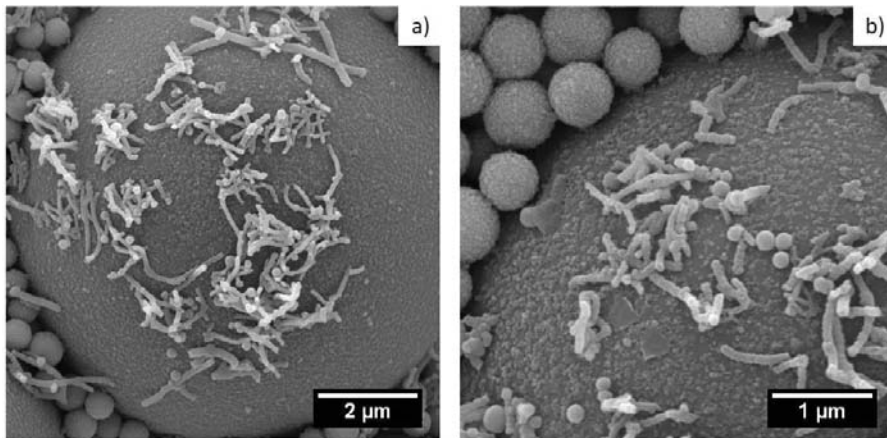


Figure S10. SEM image of silica nano-fibers deposited by one cycle of LbL deposition on BCCs substrate, showing the different components that constitute its structure: the 10 $\mu$ m spheres, 750nm particle, 20nm nanoparticles and the silica fibrils.

## Estimation of contact angles of sessile drops

To estimate the contact angles of sessile drops of water on the different surfaces we used a perturbation solution of the Bashforth-Adams equation following the protocol presented by Srinivasan and coworkers.<sup>1</sup> The profile of an axisymmetric sessile drop sitting on a surface is described by the classical equation derived by Bashforth and Adams:

$$\frac{z''}{(1+z'^2)^{\frac{3}{2}}} + \frac{z'}{x(1+z'^2)^{\frac{1}{2}}} = \frac{2}{b} + \frac{\rho \cdot g \cdot z}{\gamma_{lv}} \quad (1.1)$$

As shows in Figure S10, x and z are the lateral and vertical coordinates at the projected drop profile A, z' and z'' are respectively the first and second derivatives of z with respect to x at A,  $\rho$  is the density of the liquid, g is the acceleration due to gravity,  $\gamma_{lv}$  is the surface tension of the liquid, and  $b=(1/z''(x=0))$  corresponds to the radius of curvature at the origin O, which is located at the apex of the drop. To calculate the final contact angle, we used the approximate solution derived by Srinivasan et al. and written in the following form:

$$Z = \epsilon \left[ 1 - \cos\phi + \frac{(\pi - \phi)^2}{2} - \frac{(\pi - \phi)^2}{2} \sqrt{1 + \frac{8\epsilon^2}{3(\pi - \phi)^2}} \right] + \epsilon^3 \frac{1}{3} \left[ 1 + \cos\phi + 2 \log \frac{\epsilon}{2} + 2 \log \left[ \sqrt{\frac{8}{3} + \frac{(\pi - \phi)^2}{\epsilon^2}} + \frac{\pi - \phi}{\epsilon} \right] - 2 \log(\pi - \phi) + 2 \log \left( \cos \frac{\phi}{2} \right) \right] - f \quad (1.2)$$

to approximate the profile of the droplet. In the last equation, the different symbols appearing in the equation have the following meaning:  $Z=z/a$ ,  $\epsilon=l/a$ ;  $f=h/a$ ;  $\rho$  is the water density [1000 Kg/m<sup>3</sup>];  $\gamma_{lv}$  is the water surface tension [72 mN/m]; g is the gravity acceleration [9.81 m/s<sup>2</sup>]; h is the droplet height; l the maximum drop half-width;  $a = \sqrt{\frac{\gamma_{lv}}{\rho \cdot g}}$  is a characteristic length [m].

Figure S11

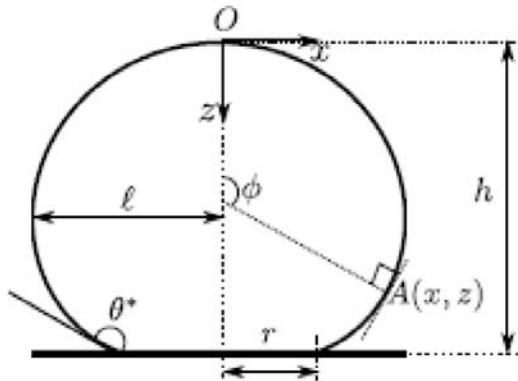


Figure S11. Schematic of an axisymmetric drop on a non-wetting substrate. For a point  $A(x, z)$  on the projected drop profile,  $x$  is the lateral coordinate,  $z$  is the vertical coordinate,  $\phi$  is the angle subtended by the normal at point  $A$  to the axis of revolution,  $\ell$  denotes the maximum drop half-width,  $r$  is the radius of the contact line,  $h$  is the height of the drop and  $\theta = \max(\phi)$  is the contact angle of the liquid drop at the three phase contact line.

**Figure S12**

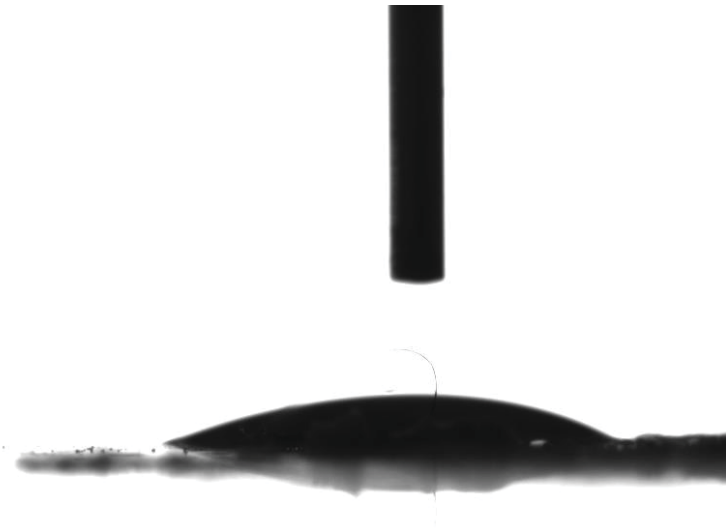


Figure S12. Contact angle measurement of a surface coated with non-hydrophobized silica nanofibers, showing the highly hydrophilic nature of the surface.

## References

1. Srinivasan, S.; McKinley, G. H.; Cohen, R. E., Assessing the accuracy of contact angle measurements for sessile drops on liquid-repellent surfaces. *Langmuir* **2011**, 27 (22), 13582-13589.